

Performance of the ATLAS Transition Radiation Tracker

Jahred Adelman on behalf of the ATLAS collaboration

Abstract

The ATLAS Transition Radiation Tracker (TRT) is a large straw tube tracking system that is the outermost of the three subsystems of the ATLAS Inner Detector (ID). With over 350,000 readout channels, the TRT provides both excellent particle identification capabilities and electron-pion separation, as well as contributing significantly to the resolution for high-pt tracks in the ID. As the instantaneous luminosity of the LHC increases, the occupancy of the TRT will increase as well. The low-occupancy tracking resolution and efficiency will be presented, as will be studies of resolution and PID at higher occupancies.



1 Introduction

The ATLAS detector [1] is a generic, multipurpose detector observing pp and heavy-ion collisions at the Large Hadron Collider at CERN. The innermost part of the ATLAS detector is the inner detector (ID), composed of the Pixel and SemiConductor Tracker (SCT) systems and the Transition Radiation Tracker (TRT). The entire ID system is immersed inside a 2T solenoid field and provides measurements of the trajectories and momenta of charged particles.

2 TRT geometry and construction

The TRT is the outermost part of the ATLAS ID, and operates primarily as a straw drift tube chamber. Charged particle ionize gas inside one of the almost 300,000 straws, creating electrons that drift towards the anode at the center of the straw, where they are read out. The TRT is divided into a barrel section at small pseudorapidity (η) and two separate endcap partitions at large η [2, 3]. All three sections have a 32-fold azimuthal symmetry in ϕ .

In the barrel, straws are 1.44 m in length and are organized parallel to the beam axis (in the z direction). The wires at the center of the straws are electrically split by a glass joint so that the two sides of the barrel detector can be read out separately. The straws are organized in groups of 73 layers, with increasing layer number corresponding to increasing radius in the detector. In order to reduce occupancy, straws in the first nine of the 73 straw layers, called “short straws”, are active only for 312 mm on either end (largest z) of the barrel. The endcaps are each divided into 14 wheels, with straws that run in the r direction (perpendicular to the beam). At smaller z , six type “A” wheels each have 16 layers of straws. At larger z , the “B” wheels have larger spacing, and only eight layers of straws per wheel. Transition radiation is created in the barrel by irregularly spaced polypropylene fibers, and in the endcap by polypropylene foils placed between each of the 160 planes of straws.

Each of the carbon Kapton straws is 4 mm in diameter and 70 μm in thickness, with carbon fiber supports [4]. The gold-plated tungsten wires at the center of each straw are 31 μm in diameter and are kept at ground with respect to the straw walls, which are kept at -1530 V. The gas circulating inside of the straws is 70/27/3% Xe/CO₂/O₂, with Xenon chosen to absorb transition radiation (TR).

3 Readout and calibration

Each of the TRT’s 353,536 channels is read out in a window of 75 ns [5]. Two separate thresholds are used to distinguish generic hits from minimum ionizing particles from those arising from TR. The low threshold (LT) is set at roughly 300 eV, while the high threshold (HT) is set at 6 KeV to detect TR. The LT signal is digitized into 24 bins of 3.12 ns over the 75 ns window; the first 0 \rightarrow 1 transition in these bins is used to define a “leading edge” (LE) that is used for tracking. The HT signal is digitized into three 25 ns wide bins over the full 75 ns window.

Before the LE can be converted into an estimated drift radius in the straw, it must be corrected for T_0 offsets [6]. These offsets account for multiple effects: time of flight in the detector, electronics and readout delays, and shifts between the LHC and ATLAS clocks. Using the third degree polynomial shown in Figure 1, the T_0 -corrected drift time relates the drift time to the drift radius in the straw. The T_0 constants are monitored run-by-run, and are updated when they drift by more than a few hundred picoseconds. As shown in Figure 2, the TRT position resolution begins to degrade once the T_0 constants have shifted by more than this amount. Typically, changes to the constants in the database are required no more than 1-2 times a month.

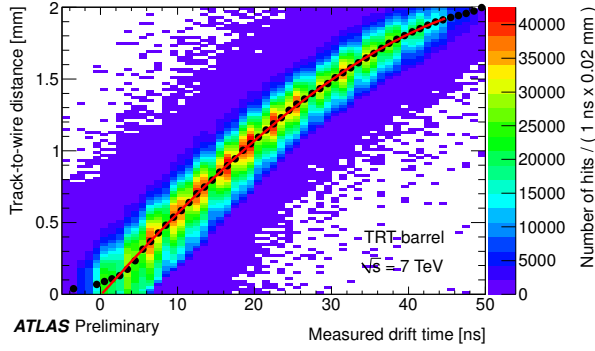


Figure 1: The r-t curve relating the corrected drift time distribution and the track-to-wire distance [6].

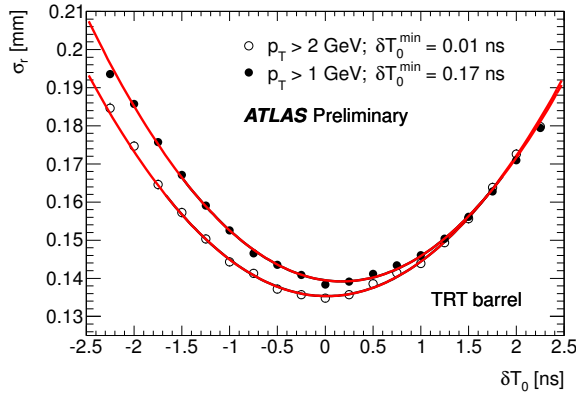


Figure 2: Position resolution width in the TRT as a function of shifts in T_0 constants [6].

4 Performance

With a large lever arm in the ID and roughly 30 hits per track, the TRT contributes significantly to the ID momentum resolution, especially at high p_T . In addition, the detection of significant TR allows the TRT to provide excellent pion-separation [7]. Figure 3 shows the distribution of the fraction of tracking hits with HT hits attached, separately for pions and electrons. Using this distribution, one can significantly reject pions for high electron efficiency. For 90% electron efficiency, 1-2 order-of-magnitude pion rejection can be obtained. The variation in η is due to varying amounts of radiator material over the detector. In particular, the B wheels of the endcap have more radiators and produce larger amounts of TR. The performance is worse in the barrel-endcap transition, due to having fewer TRT hits on track.

Figure 4 shows track position residuals as a function of track p_T . At low p_T (particularly in the endcaps), the residuals are sensitive to scattering off of material in the detector. Scattering can also be seen in the residual maps, shown in Figure 5. Here, the width of the residuals can be seen to increase as particles pass through more material, particularly at large radius and large Z in the detector. The width of the residual distribution is best in the short straws. This is due to the larger average incidence angle (a geometrical effect), a higher LT setting (the LT is set manually, so that the noise level in the shorter straws is the same as the level in the longer straws), as well as material effects.

The excellent, better-than-design resolution was a result of the precision alignment of the detector [8], as shown in Figure 6. Without the wire-by-wire alignment, significant structure is seen in the mean of the position residuals. The improved alignment removes this structure, and significantly improves the TRT resolution.

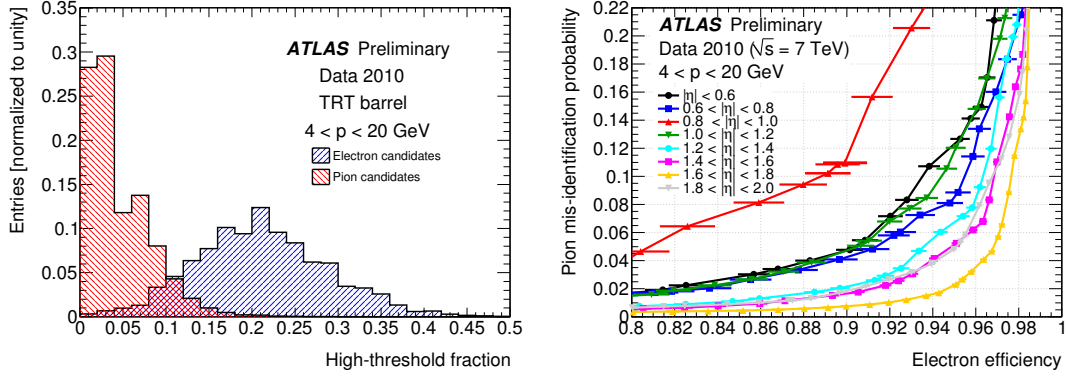


Figure 3: Left: HT fraction for electron and pions in the barrel. Right: Pion rejection for a given electron efficiency for different η regions in the detector [7].

The position residuals as a function of the number of reconstructed primary vertices are shown in Figure 7. Only tracks above 10 GeV are used so as to remove any dependence on the increased number of soft tracks occurring with every extra minimum bias interaction. Though a rise is seen, it is very small, corresponding to just a few percent increase in residual width.

Another important performance metric is the track hit efficiency, shown in Figure 8. The efficiency is calculated as a function of track-to-wire distance; the efficiency decreases near the straw edges due to decreased path length in the straw. Very close to the straw edge, tracking uncertainties can also appear as a straw inefficiency.

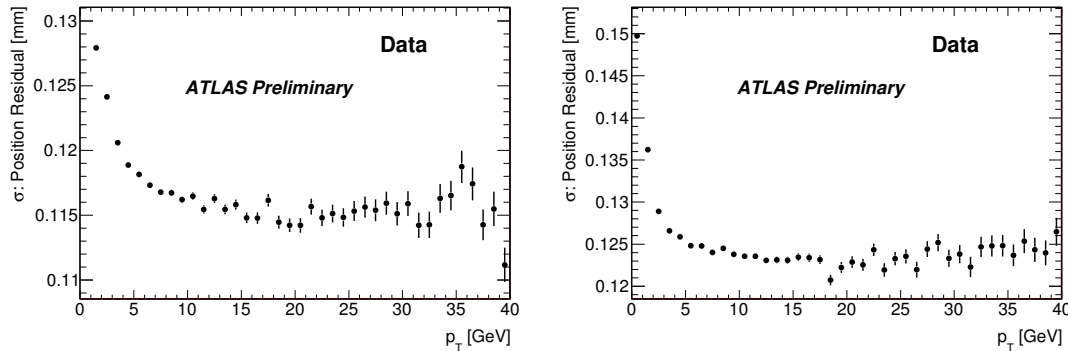


Figure 4: Position residual width as a function of track p_T , for the barrel (left) and endcap (right) [9].

The valid leading edge distribution (first $0 \rightarrow 1$ transition) and trailing edge (last $1 \rightarrow 0$ transition) is shown in Figure 9. The LHC is currently running with 50 ns bunch spacing. Out-of-time hits are easily handled with this bunch spacing by requiring both that the uncorrected LE is not too large (it must be less than 60 ns, which rejects out-of-time hits from late bunch crossings) and also requiring a valid $0 \rightarrow 1$ transition (which rejects hits from early bunch crossings). These cuts have only a minimal effect on TRT efficiency, but are very efficient at rejecting out-of-time pileup. If the LHC moves to the nominal 25 ns bunch spacing next year, more sophisticated cuts will have to be made.

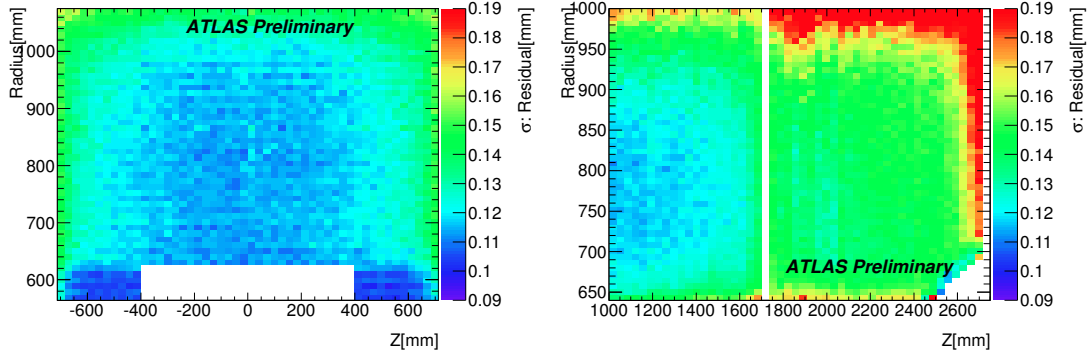


Figure 5: Position residual width for tracks with $p_T > 2$ GeV as a function of radius and Z in the detector, shown for the barrel (left) and endcap side A (right) [9].

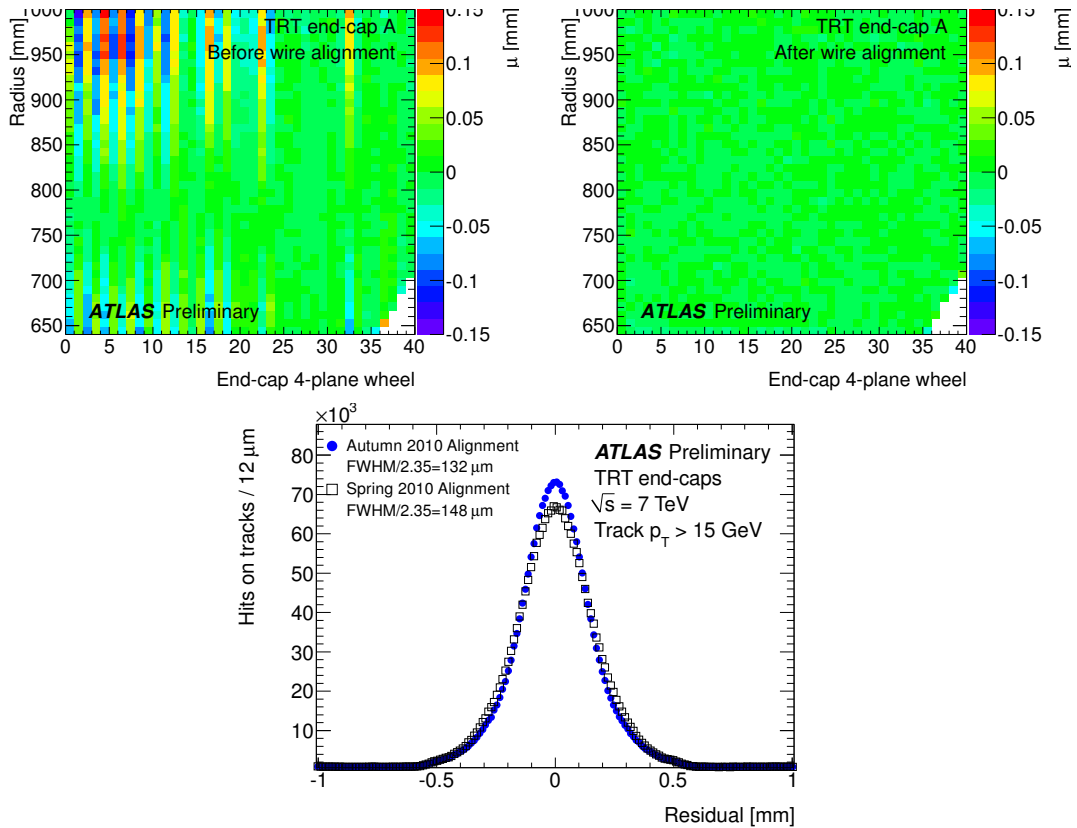


Figure 6: Mean of the position residuals in endcap side A as a function of radius and 4-plane wheel before (top left) and after (top right) the wire-by-wire alignment procedure. The improvement in residuals is shown in the bottom plot [6].

5 Occupancy

Figure 10 shows the occupancy in the detector as a function of barrel straw layer and endcap wheel number. The occupancies are shown for different number of primary vertices in the event. At 10 primary vertices, the LL occupancy in regions of the barrel (endcap) can reach over 30 (20)%. The HL occupancy in these regions is over 2.5% in the barrel and over 1.6% in the endcap. The change in occupancy as each

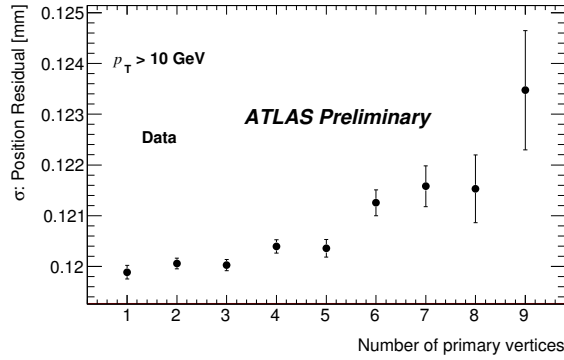


Figure 7: Position residuals for high- p_T tracks as a function of the number of reconstructed primary vertices in the event [9].

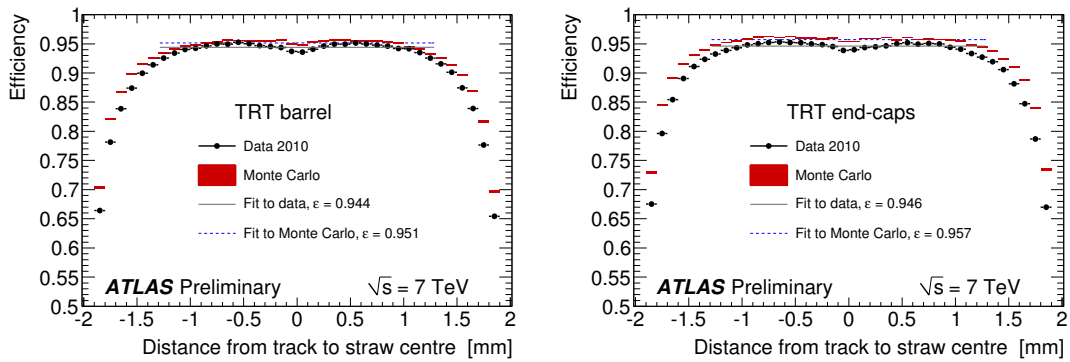


Figure 8: TRT hit efficiency as a function of track distance to the wire in the straw for barrel (left) and endcap (right) [9].

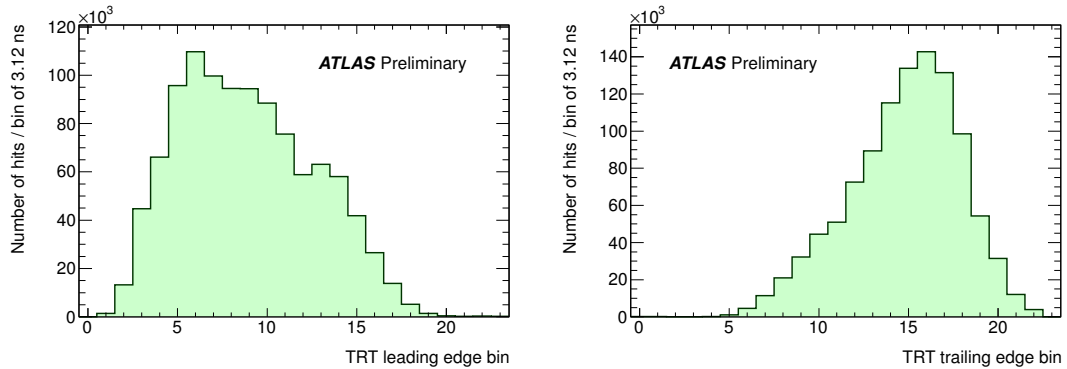


Figure 9: Leading edge (left) and trailing edge (right) distributions [6].

additional vertex is found is shown in Figure 11. The points largely lie on top of one another, indicating that at these instantaneous luminosities, pileup is not yet a major issue.

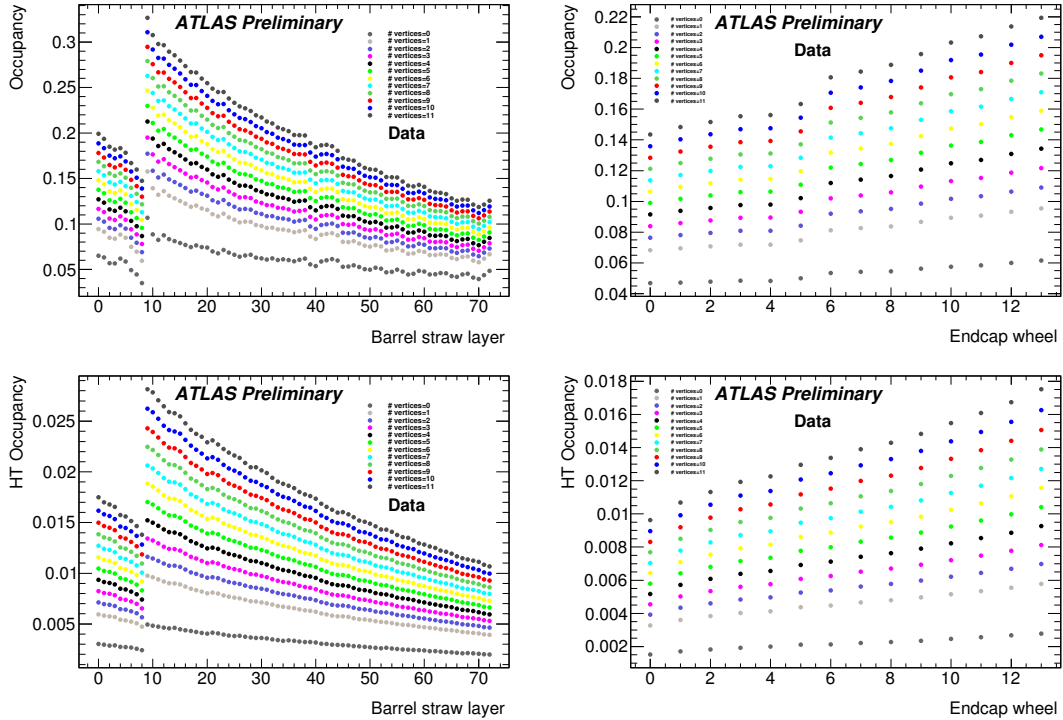


Figure 10: Occupancy in the barrel (left) and endcap (right) shown as a function of straw layer and endcap wheel. The top plots show the LL occupancy, and the bottom plots show the HL occupancy. The colors in each plot are for different numbers of reconstructed primary vertices in the event. The lowest occupancy points have zero reconstructed primary vertices, and the highest occupancy points have 11 such vertices [9].

6 Conclusion

The TRT is a key component not only of the ATLAS Inner Detector, but also of the entire ATLAS experiment. Its long lever arm and large number of hits on track enable significant improvement to the ID momentum resolution, and the detection of transition radiation provides significant electron-pion separation. The occupancy of the TRT continues to rise as the LHC provides higher instantaneous luminosities, but the TRT is prepared and poised to continue to contribute to the ATLAS physics program.

7 Bibliography

References

- [1] The ATLAS Experiment at the CERN Large Hadron Collider, JINST **3**, S08003 (2008).
- [2] ATLAS TRT Barrel Detector, JINST **3**, P02014 (2008).
- [3] The ATLAS TRT end-cap detectors, JINST **3**, P10003 (2008).
- [4] The ATLAS Transition Radiation Tracker (TRT) proportional drift tube: design and performance, JINST **3**, P02013 (2008).
- [5] The ATLAS TRT electronics, JINST **3**, P06007 (2008).

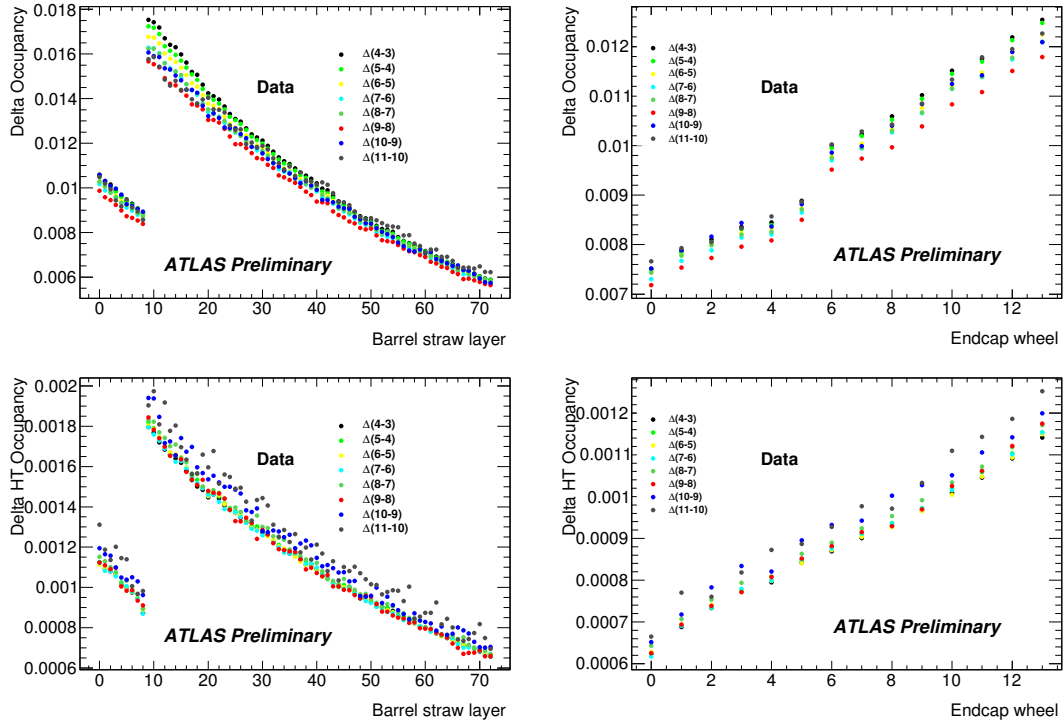


Figure 11: Changes in occupancy in the barrel (left) and endcap (right), shown as a function of straw layer and endcap wheel. The top plots show the changes in LL occupancy, and the bottom plots show the changes in HL occupancy. The colors in each plot correspond to changes in occupancy when comparing events with different numbers of reconstructed primary vertices in the event [9].

[6] Calibration of the ATLAS Transition Radiation Tracker, <https://cdsweb.cern.ch/record/1330712>.

[7] Particle Identification Performance of the ATLAS Transition Radiation Tracker, <https://cdsweb.cern.ch/record/1383793>.

[8] Alignment of the ATLAS Inner Detector Tracking System with 2010 LHC proton-proton collisions at $\sqrt{s} = 7$ TeV, <https://cdsweb.cern.ch/record/1334582>.

[9] <https://twiki.cern.ch/twiki/bin/view/AtlasPublic/TRTPublicResults>